Binuclear oxidative addition of Sb-Cl bonds : a facile synthetic route to main group transition element clusters and rings

Li, Ying-Zhou; Ganguly, Rakesh; Leong, Weng Kee

Binuclear Oxidative Addition of Sb-Cl Bonds: A Facile Synthetic Route to Main Group-Transition Element Clusters and Rings

Ying-Zhou Li, Rakesh Ganguly and Weng Kee Leong*

Division of Chemistry & Biological Chemistry, Nanyang Technological University, 21 Nanyang Link, Singapore, 637371

ABSTRACT: Binuclear oxidative addition of Sb-Cl bonds with the clusters $Os_3(CO)_{11}(NCCH_3)$, **1**, or $Os_3(CO)_{10}(NCCH_3)_2$, **2**, was found to be an effective synthetic route to organometallic clusters and rings containing μ_2-SbPh$_2$ or μ_3-SbPh moieties. Thus the reaction of SbPh$_2$Cl with **1** afforded the tetranuclear ring $Os_3(CO)_{11}(Cl)(\mu\text{-SbPh}_2)$, **3**, while its reaction with **2** afforded the pentanuclear ring $Os_3(CO)_{10}(Cl)_2(\mu\text{-SbPh}_2)_2$, **6**. In each case, two or three isomeric products were isolated depending on the reaction conditions. The analogous reaction of SbPhCl$_2$ with **1**, on the other hand, afforded the spiked triangular cluster $Os_3(CO)_{11}(Cl)_2(\mu_3\text{-SbPh})$, **7**, which also existed as two isomers. Pathways for these reactions have been proposed, and the experimental and computational evidence presented.

Introduction

Organometallic clusters containing heavier main group and transition metal elements are of interest because of their distinct structural and reactivity patterns, which are unlike those of their homometallic analogues.[1] For many years now, we have been interested in the preparation and reactivity studies of osmium-antimony clusters; these show different reactivity

patterns from those containing its lighter congeners, phosphorus and arsenic.[2] One aspect of interest is that of synthesis – there is a general lack of readily available antimony ligands and efficient synthetic methodologies, and the predictability of products in many of these, for example, thermolytic reactions, are poor. In a recent paper, we reported the oxidative addition of osmium clusters across the Sb-H and Sb-Sb bonds of $SbPh_2H$ and Sb_2Ph_4, respectively, as an efficient method to prepare osmium-antimony clusters containing the μ_2-$SbPh_2$ moiety.[3] Of particular interest was that these binuclear oxidative addition reactions resulted in the cleavage of a metal-metal bond to form an Os_3Sb ring. Such metal-metal bonded ring compounds are relatively rare.[4] We thus became interested in exploring the possibility of utilizing binuclear oxidative addition as a synthetic route to this class of compounds.

The halostibines are attractive as antimony precursors since they are among the more readily available organoantimony compounds. For instance, they are more stable than the hydrostibines. Even so, the antimony-halogen bond is expected to be susceptible to oxidative addition, and the halogen substituent also increases the Lewis acidity of the Sb center.[5] Only a relatively small number of organotransition metal complexes containing halostibine ligands have been synthesized and characterized spectroscopically and crystallographically, all of which were mono- or di-nuclear transition metal carbonyls in which the halostibine acted as terminal ligands.[6] We therefore decided to explore the reactions of halostibines with trinuclear osmium carbonyls as a possible synthetic route to metal-metal bonded ring compounds. The results of our investigations are reported here.

Results and discussion

In contrast to the hydrostibines (SbPh$_2$H) and distibines (Sb$_2$Ph$_4$), the reaction of the halostibines (SbPh$_2$Cl and SbPhCl$_2$) with the lightly-stabilised triosmium carbonyl clusters Os$_3$(CO)$_{11}$(NCCH$_3$), **1**, and Os$_3$(CO)$_{10}$(NCCH$_3$)$_2$, **2**, proceeded at a slower rate and the products obtained were more stable. Thus the reaction of **1** and SbPh$_2$Cl in DCM afforded a compound **A** which could not be separated on silica gel. A comparison of its IR spectroscopic characteristics with those of the known compound Os$_3$(CO)$_{11}$(SbPh$_3$),[7] suggested that it was the substitution product Os$_3$(CO)$_{11}$(SbPh$_2$Cl) (Figure S1). In a more polar solvent such as acetone, **A** converted to a pair of isomeric ring clusters Os$_3$(CO)$_{11}$(Cl)(μ-SbPh$_2$), **3a** and **3b**, in which the Cl atom occupies an equatorial and axial position, respectively (Scheme 1). The yields for the two products totaled > 80%. Both these clusters have been characterized crystallographically, and the ORTEP diagrams depicting their molecular structures are given in Figures 1 and 2, respectively.
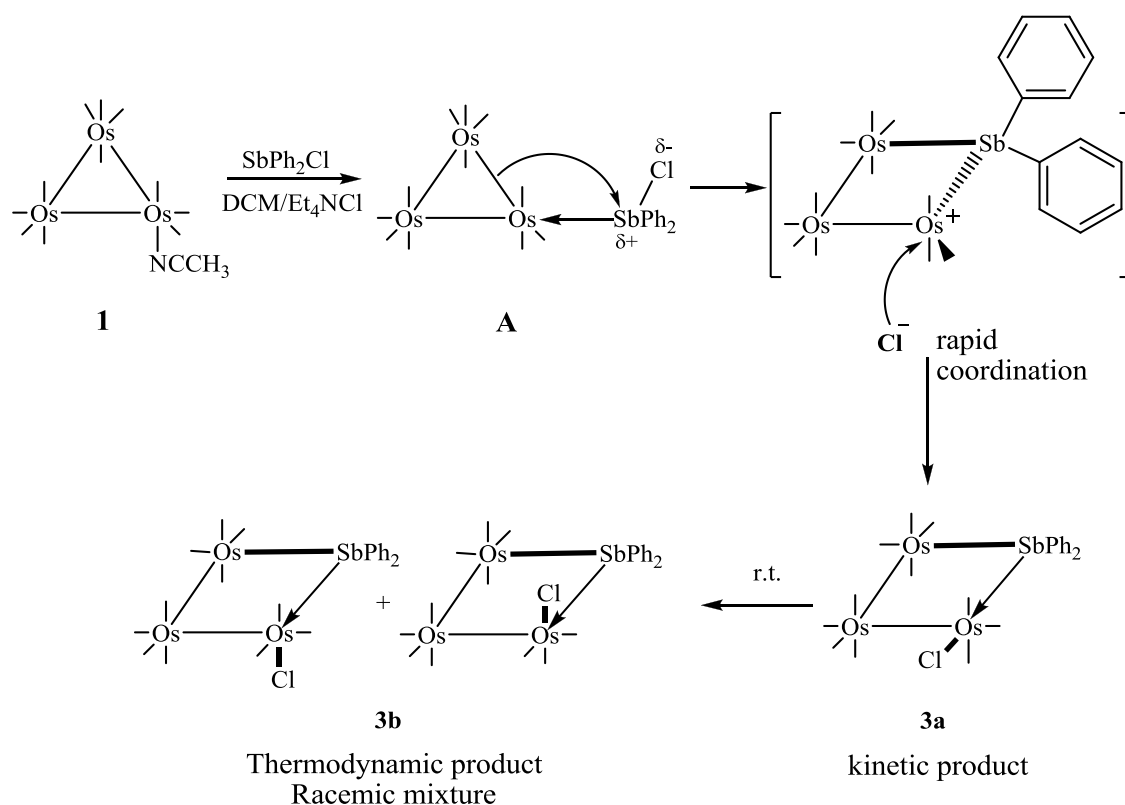
Scheme 1

The *trans* geometry of the Cl and SbPh$_2$ moieties is similar to that observed in some other structurally characterised products resulting from oxidative addition across Si-Cl,[8] Sn-Cl,[9] or B-Cl bonds.[10] Compared to the large number of examples known for the oxidative addition of C-X, Si-X (X = halide), Ge-Cl,[11] and Sn-Cl,[12] bonds to transition metals, the oxidative addition of pnictogen-halogen bonds to transition metals are very rare. The few examples known include the oxidative addition of a P-Cl bond to a dimolybdenum carbonyl,[13] and of a Bi-Cl bond to Pt(0).[14] To the best of our knowledge, this is the first example of oxidative addition of the Sb-Cl bond to a transition metal.
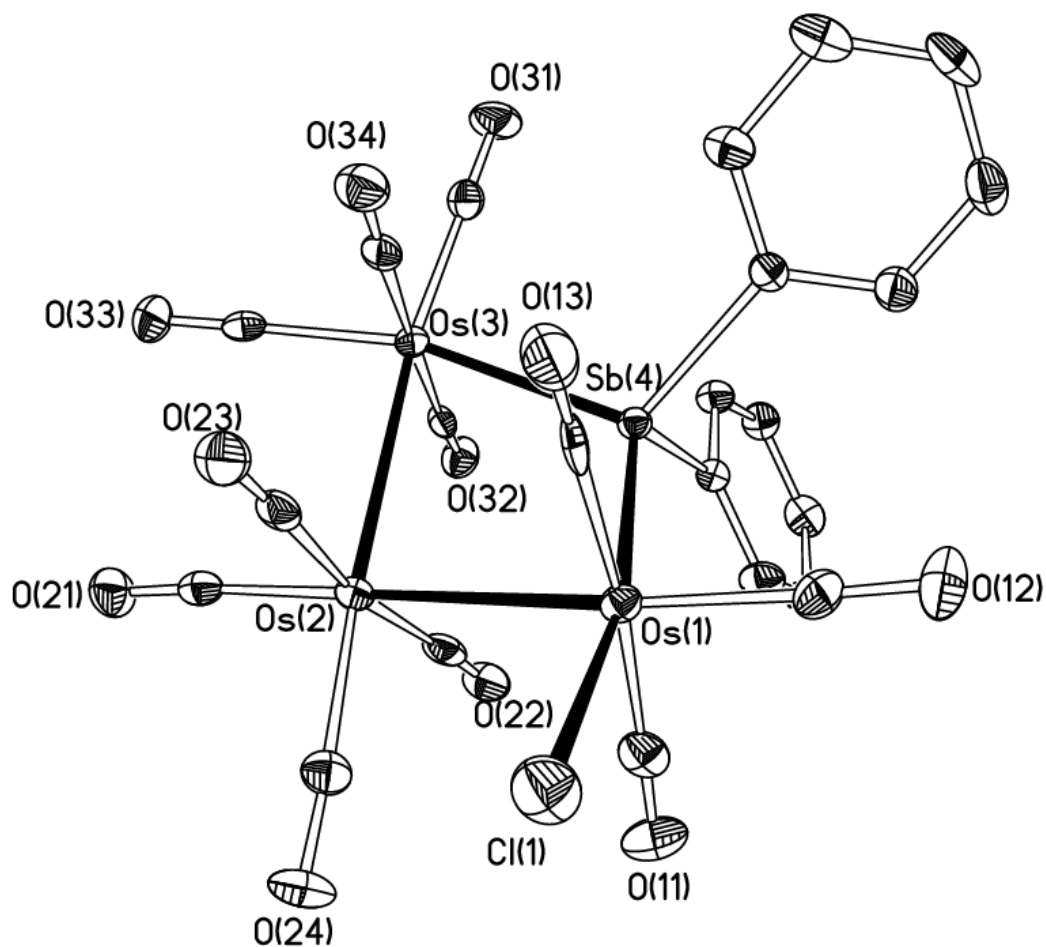
Figure 1. ORTEP diagram of the molecular structure of **3a**. Hydrogen atoms have been omitted

and the thermal ellipsoids are drawn at the 50% probability level.
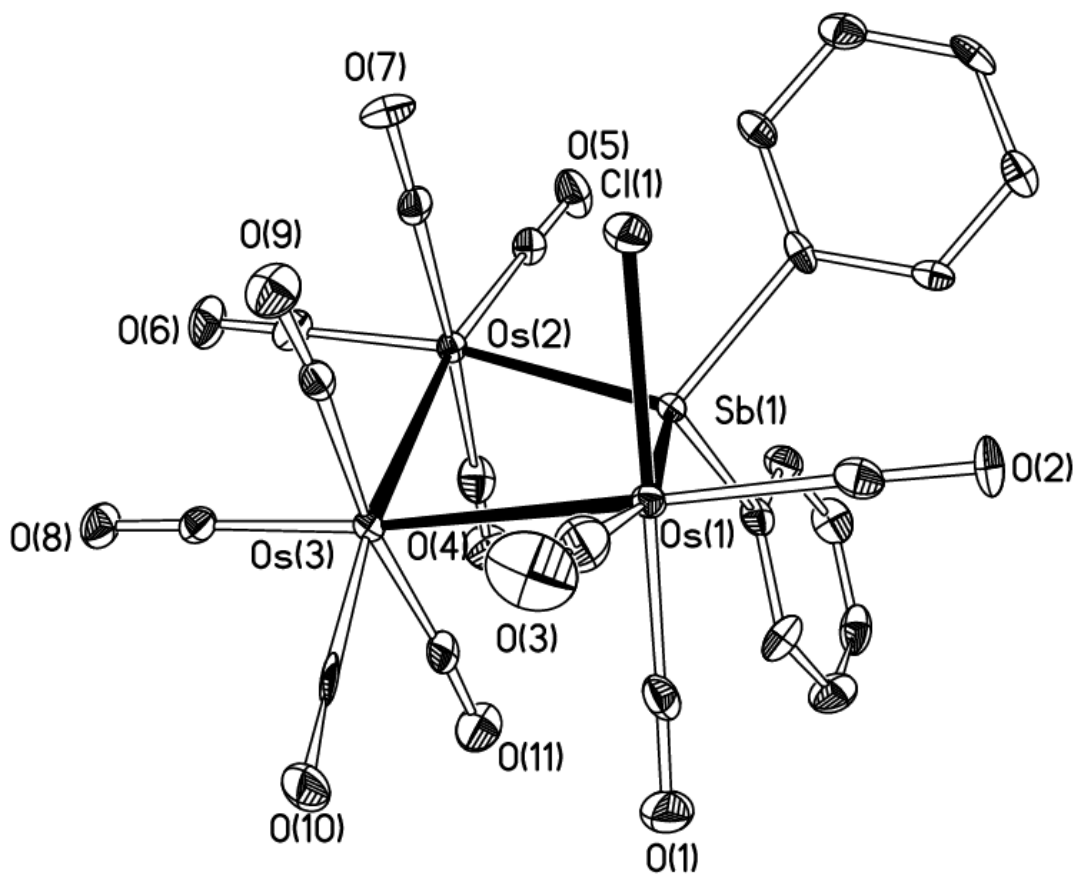
Figure 2. ORTEP diagram of the molecular structure of **3b**. Hydrogen atoms have been omitted and the thermal ellipsoids are drawn at the 50% probability level.

A solution of **3a** gradually converted to **3b** on standing (Figure S2), suggesting that the former was the initial product and the latter the thermodynamically more stable product; **3b** has a *fac* arrangement of the $Os(CO)_3$ moiety, which avoids having a mutually *trans* arrangement of two strong π-accepting CO ligands, as opposed to a less favourable *mer* arrangement in **3a**. The isomerisation presumably proceeded via a "turnstile" mechanism. The computed free energies, based on DFT calculations at the B3LYP/LANL2DZ level of theory, also showed that **3b** was more stable by ~35 KJ/mol. Monitoring the reaction of **1** and $SbPh_2Cl$ by ^{1}H NMR spectroscopy showed only the presence of resonances attributable to Ph_2SbCl, **A**, **3a** and **3b**

(Figures S3 and S4). Thus although **3b** is the Cl analogue of the previously reported cluster Os$_3$(CO)$_{11}$(H)(μ-SbPh$_2$), **3'**, which was obtained from the reaction of **1** with SbPh$_2$H,[3] this observation suggested that the formation of **3a/b** followed a different pathway. In that study, the formation of **3'** was shown to proceed through an intramolecular rearrangement from the intermediate Os$_3$(CO)$_{11}$(μ-H)(SbPh$_2$), which was trapped with W(CO)$_5$(NCCH$_3$). In the reaction with SbPh$_2$Cl, however, no such analogue, *viz.*, Os$_3$(CO)$_{11}$(μ-Cl)(SbPh$_2$), was trapped using the same strategy.

That the conversion of **A** to **3a/b** was accelerated in a more polar solvent was also inconsistent with an intramolecular rearrangement. The conversion was also accelerated by the addition of one equivalent of Et$_4$NCl to the reaction (with either DCM or THF as solvent), while an analogous reaction without the addition of salt remained as unconverted **A** even after a long time. The bromo analogue of **3b**, *viz*, Os$_3$(CO)$_{11}$(Br)(μ-SbPh$_2$), **3c**, could be isolated if Et$_4$NBr was used as the additive; **3c** has also been fully characterized, including by a single crystal X-ray diffraction analysis. We therefore propose that the reaction proceeded via an S$_N$2-type binuclear oxidative addition mechanism (Scheme 1), i.e., involving a cationic cluster species. This oxidative addition pathway is usually adopted for polarized substrates such as alkyl halides and halogens.[15] The observed geometries of **3a** and **3c**, with the halogen and SbPh$_2$ moieties adopting a mutually *trans* arrangement, are also consistent with the proposed mechanism.

Selected bond parameters for clusters **3a-c** are collected in Table 1, with the common atom labeling scheme shown.

Table 1. Selected bond parameters and common atom labeling scheme for **3a-c**.
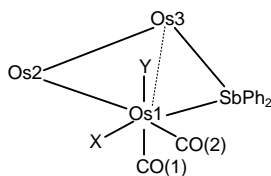
| Bond length (Å)	3a	3b	3c
	X = Cl Y = CO	X = CO Y = Cl	X = CO Y = Br
Os1-Os2	2.9833(2)	2.9696(5)	2.9849(3)
Os2-Os3	3.0021(3)	3.0254(5)	3.0264(4)
Os1…Os3	4.275	4.330	4.342
Os1-Sb	2.6002(3)	2.6406(6)	2.6455(6)
Os3-Sb	2.6714(3)	2.6731(6)	2.6887(5)
Os1-X	2.4466(14)	3.084*	3.093*
Os1-Y	3.076*	2.467(2)	2.5981(7)
Os1-CO(1)*	3.073	3.009	3.027
Os1-CO(2)*	3.025	3.067	3.052
Dihedral angle[†] (°)	146.8	150.8	150.6

*The values given are sum of the Os-C and C-O bond lengths.

[†] Between the Os1Os2Os3 and Os1Os3Sb planes.

The Os_3Sb ring is puckered, the dihedral angle between the Os1Os2Os3 and Os1Os3Sb planes being ~150°. In **3b** and **3c**, the Sb atom lies off the Os_3 plane on the side away from Y. The reason for this is not clear, especially for **3a**, but in all three clusters, the $Os(CO)_2(X)(Y)$ moiety is rotated so that, for instance, Y is no more clearly axially orientated with respect to the Os_3 plane. This suggests that the presence of the halide ligand on Os1 has a significant electronic effect on that Os atom, as is also apparent from the observation that both the Os1-Os2 and Os1-Sb bond lengths are shorter than the corresponding bonds to Os3. The Os1-Sb bond, which is *trans* to X = Cl, is the shortest of the Os-Sb bond lengths; this can be attributed to the reduced *trans* influence of Cl compared to a CO for the others. This, however, cannot explain the same

shortening, albeit to a smaller extent, in **3b** and **3c**. The reduced *trans* influence of Cl is also apparent in the effect it has on the sum of Os-C and C-O bond lengths for Os1-CO(1) in **3b** and **3c**, which are very short (~3.01 and 3.03 Å, respectively); we had advocated the use of this sum of bond lengths rather than either of the individual bond parameters as a more reliable measure of the metal-carbonyl bonding interaction.[2b,f,16]

Thermolysis of **3b** (refluxing DCE) led to decarbonylation to afford the chloro-bridged cluster $Os_3(CO)_{10}(\mu\text{-}Cl)(\mu\text{-}SbPh_2)$, **4**. This cluster has also been characterized by a single crystal X-ray diffraction analysis, and an ORTEP diagram of its molecular structure, together with selected bond parameters, is shown in Figure 3. The long Os(1)...Os(3) vector (3.557 Å) shows that there is no bond between Os(1) and Os(3). Treatment of cluster **3b** with Na_2CO_3 in a THF/H_2O solvent mixture afforded the known hydride-bridged cluster $Os_3(CO)_{10}(\mu\text{-}H)(\mu\text{-}SbPh_2)$, **5**, as the sole separable product, in a moderate yield.[17,2d] Attempts to optimize this reaction using other bases, such as NaOH and KOH, gave no significant improvement in yield. Cluster **5** was presumably formed via the Hieber base reaction.
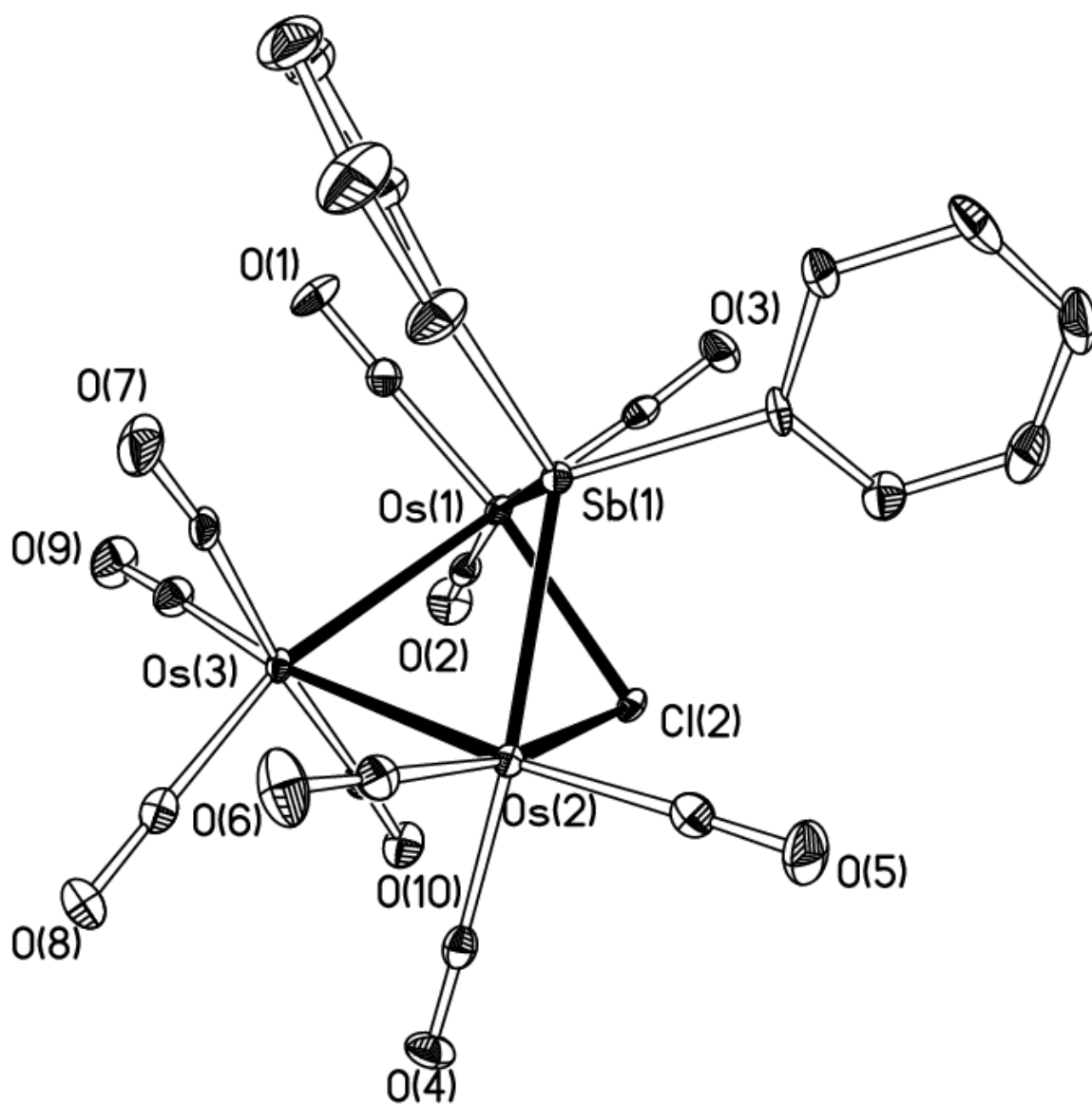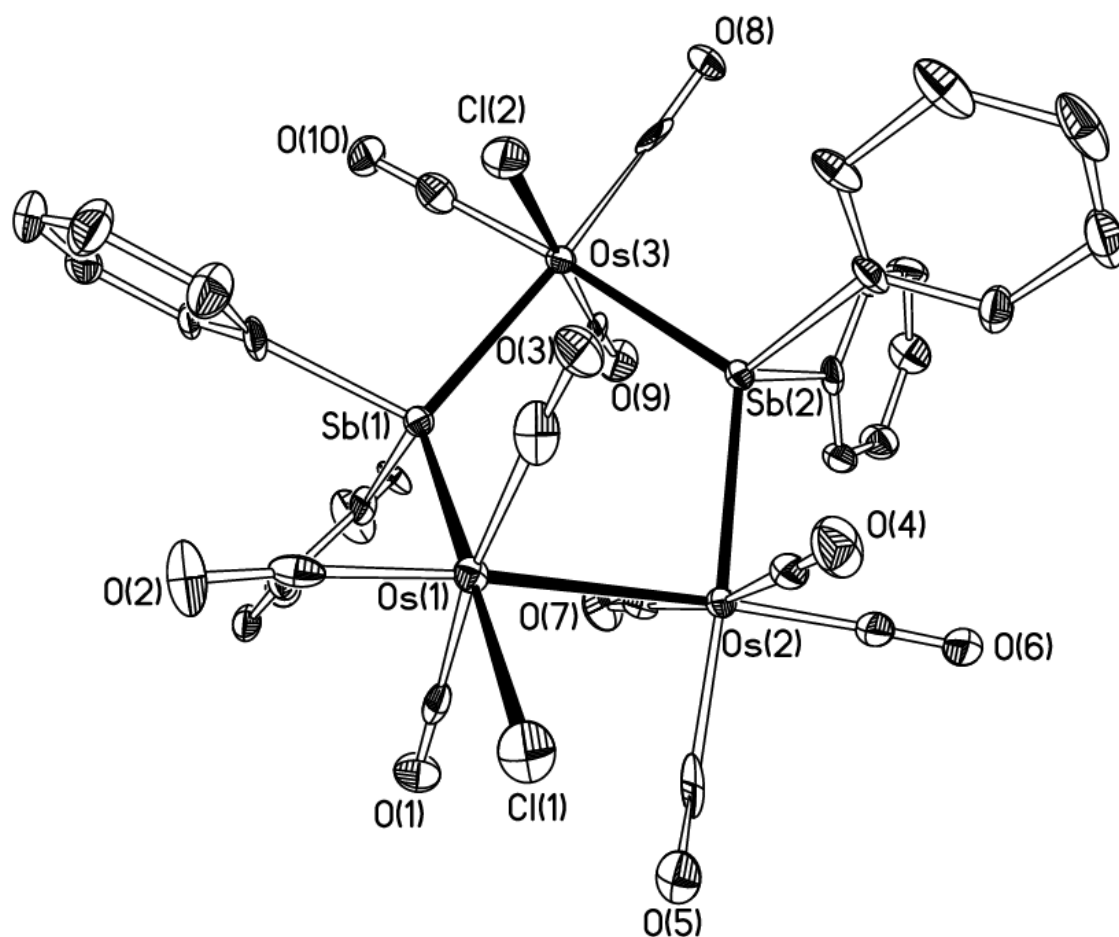
Figure 3. ORTEP diagram of the molecular structure of **4**. Hydrogen atoms have been omitted

and the thermal ellipsoids are drawn at the 50% probability level. Selected bond distances (Å):

Os(1)-Sb(1) = 2.6558(4), Os(2)-Sb(1) = 2.6613(5), Os(1)-Os(3) = 2.9083(3), Os(2)-Os(3)

= 2.9085(3), Os(1)-Cl(2) = 2.500(1), Os(2)-Cl(2) = 2.515(1).

The analogous reaction of **2** and one equivalent of SbPh$_2$Cl in DCM at room temperature led to **4**, but the use of two equivalents of SbPh$_2$Cl afforded a series of isomeric five-membered rings **6a**, **6b** and **6c**, depending on the reaction conditions. These rings are the result of two consective binuclear oxidative additions, and are in distinct contrast to the corresponding reaction with SbPh$_2$H which furnished a complex mixture and a trace amount of the cluster Os$_3$(CO)$_{10}$(μ-SbPh$_2$)$_2$.[2d] We have found that all the three ring compounds **6** were formed via **4** (Figures S9). The major isomer formed at room temperature was **6a**, together with a small amount of **6b**, whereas at elevated temperature (85 °C), **6b** and **6c** were the major products; the results are summarised in Scheme 2.
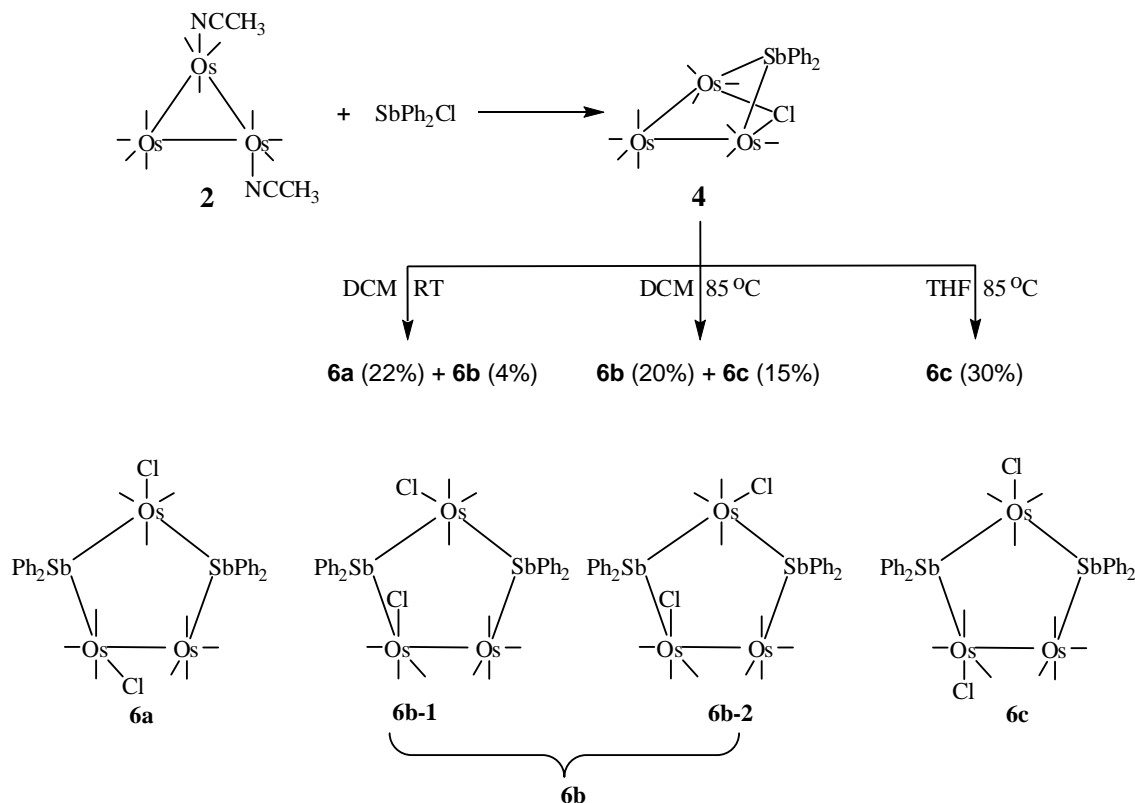

Scheme 2

All three rings have been fully characterised, including by single crystal X-ray crystallographic studies; their ORTEP diagrams, and selected bond parameters, are given in Figures 4-6, respectively. Such pentanuclear Os_3Sb_2 rings have previously been obtained via nucleophilic addition that resulted in metal-metal bond opening of a complex and not readily available osmium-antimony cluster.[18] The isomers **6a-c** differ in the relative stereochemistry about the two $Os(CO)_3Cl$ moieties; they have a *fac,mer*, *mer,fac* and *fac,fac* arrangement of the carbonyls, respectively, where the first designates the CO arrangement on the isolated $Os(CO)_3Cl$ unit. In addition, it was found that the isolated TLC band corresponding to **6b** actually comprised two stereoisomers, labelled as **6b-1** and **6b-2**. This was apparent from the ^{1}H NMR spectrum, which showed two sets of resonances with an integration ratio of *ca.* 6:4 (Figure S17). The crystal used in the crystallographic study exhibited disorder, which was interpreted as comprising mainly one stereoisomer (**6b-1**). In contrast, the ^{1}H NMR spectra of **6a** and **6c** both showed four doublets and one multiplet signals in the aromatic region, corresponding to the four chemically nonequivalent Ph rings and consistent with the solid-state structures.

Figure 4. ORTEP diagram of the molecular structure of **6a**. Hydrogen atoms have been omitted and the thermal ellipsoids are drawn at the 50% probability level. Selected bond distances (Å): Os(1)-Os(2) = 2.9615(5), Os(1)-Sb(1) = 2.6585(7), Os(2)-Sb(2) = 2.6956(8), Os(3)-Sb(1) = 2.7010(9), Os(3)-Sb(2) = 2.7028(8), Os(3)-Cl(2) = 2.437(3), Os(1)-Cl(1) = 2.456(3).
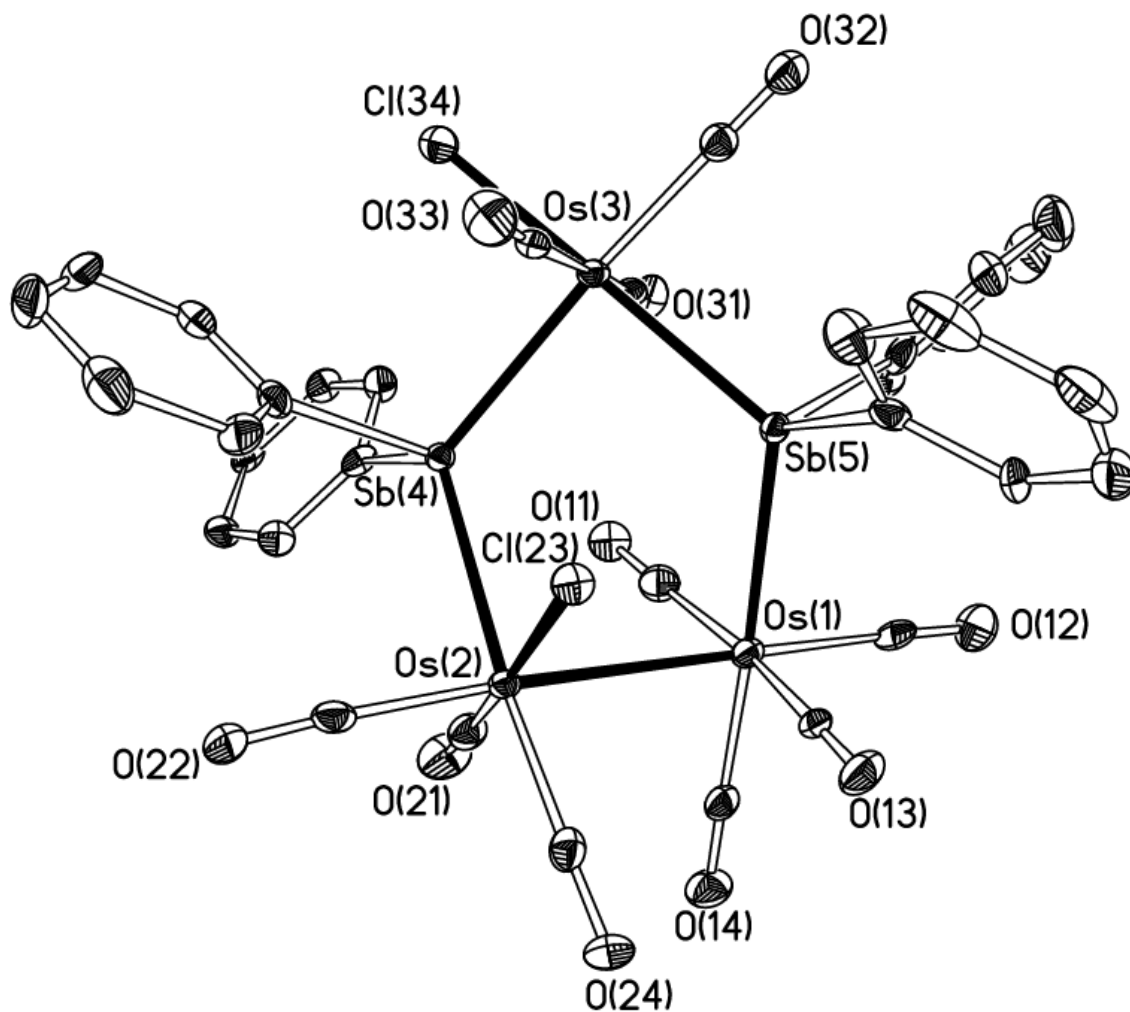
Figure 5. ORTEP diagram of the molecular structure of **6b**. Hydrogen atoms have been omitted

and the thermal ellipsoids are drawn at the 50% probability level. Selected bond distances (Å):

Os(1)-Os(2) = 2.9563(4), Os(1)-Sb(5) = 2.7060(6), Os(2)-Sb(4) = 2.7099(5), Os(3)-Sb(4)

= 2.6901(5), Os(3)-Sb(5) = 2.6659(5), Os(3)-Cl(34) = 2.447(3), Os(2)-Cl(23) = 2.433(4).
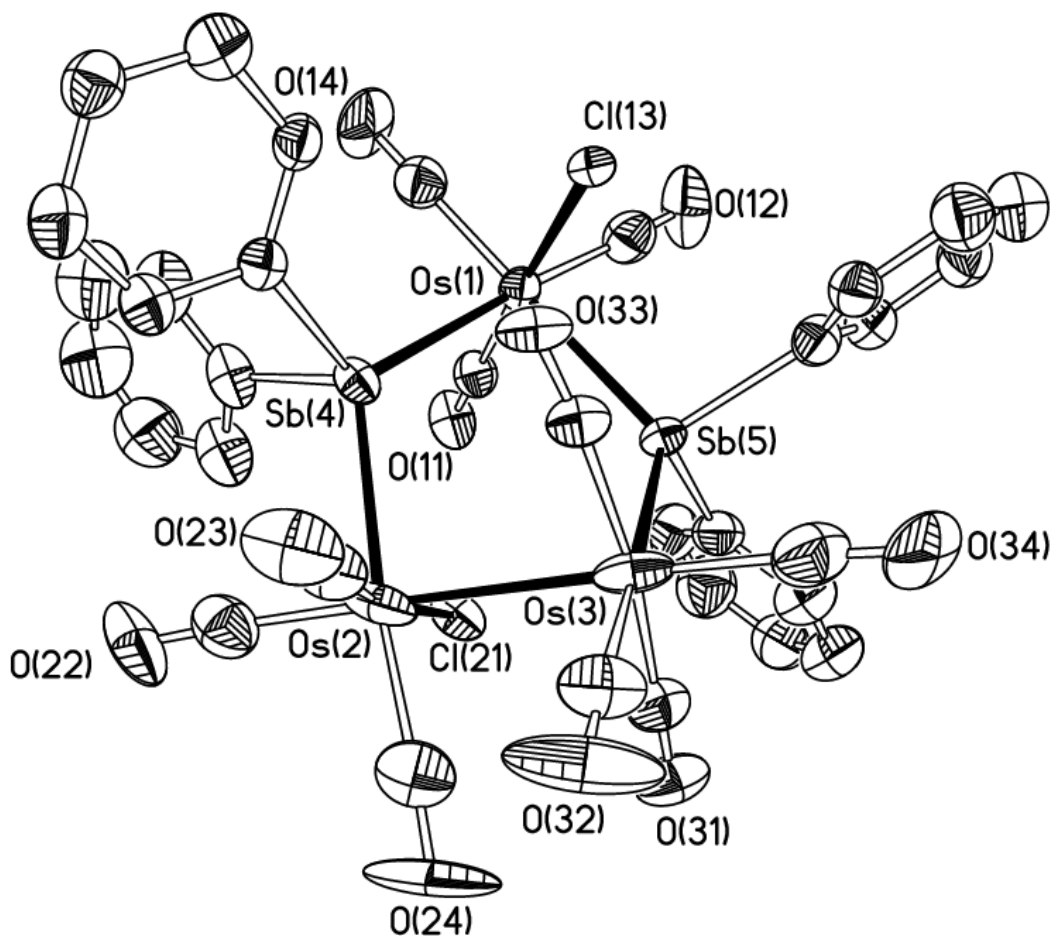
Figure 6. ORTEP diagram of the molecular structure of **6c**. Hydrogen atoms have been omitted and the thermal ellipsoids are drawn at the 50% probability level. Selected bond distances (Å): Os(2)-Os(3) = 2.956(1), Os(1)-Sb(4) = 2.6981(9), Os(1)-Sb(5) = 2.695(1), Os(2)-Sb(4) = 2.706(1), Os(3)-Sb(5) = 2.7058(9), Os(2)-Cl(21) = 2.414 (5), Os(1)-Cl(13) = 2.433(5).

The presence of two stereoisomers in **6b** was also corroborated by a similar observation with the *p*-tolyl analogue, **Tolyl-6b**, which was prepared from the reaction of **2** and (*p*-tolyl)$_2$SbCl; the analogue of **6c**, *viz.*, **Tolyl-6c**, was similarly obtained from the reaction carried out at 85 °C. Both these clusters have also been characterised crystallographically (Figure S22 and S24). The ^{1}H NMR spectrum of **Tolyl-6b** also suggested the presence of two isomers,

although the expected eight methyl resonances were not well separated. Nevertheless, the crystal chosen for X-ray crystallographic analysis exhibited disorder which could be interpreted as due to the presence of the two corresponding stereoisomers, **Tolyl-6b-1** and **Tolyl-6b-2**, in the same ratio (4:6) as was found in the NMR spectrum. An EXSY spectrum taken of **Tolyl-6b** did not show any interconversion on the NMR timescale (Figure S21).

While the reaction at elevated temperature (80 °C) did favour the formation of **6b** over **6a**, standing a solution (DCM, DCE or THF) of **6a** led to its conversion to an unidentified species **B**, which quickly converted (essentially quantitatively) upon heating, to **6c** (Figure S10). In contrast, the conversion of **6b** to **6c** was found to be solvent dependent; there was hardly any conversion in DCM or DCE (85 °C for 12h) while the conversion was nearly quantitative in THF. The latter is also consistent with the observation that only **6c** was obtained in the reaction of **2** and Ph_2SbCl in THF at 85 °C. The solvent dependence suggests that a dissociative mechanism for the isomerisation of **6b** to **6c** may be operative. All these interconversions are consistent with the computed free energies, which show that **6c** is the most stable, with **6b-1** at 30.2 KJ/mol above it, followed by **6b-2** (a further 0.6 KJ/mol) and finally **6a** (another 1.6 KJ/mol).

The reaction of **1** with $SbPhCl_2$ in DCM over 48h at room temperature afforded *mer*-$Os_3(CO)_{11}(Cl)_2(\mu_3\text{-}SbPh)$, **7a**. A prolonged reaction time (>10 d) led to isomerisation of **7a** into *fac*-$Os_3(CO)_{11}(Cl)_2(\mu_3\text{-}SbPh)$, **7b** (Figure S11), together with the formation of another product *mer*-$Os_3(CO)_{11}(Cl)(Ph)(\mu_3\text{-}SbPh)$, **8**, in minor amounts. The observed isomerization is consistent with a DFT calculation which shows that **7a** lies about 45 KJ/mol above **7b**. All

three clusters have been fully characterized, including by single crystal X-ray crystallography. The ORTEP diagrams depicting their molecular geometry are given in Figures 7-9, respectively, and selected bond parameters are collected in Table 2, together with a common atom labeling scheme.

Table 2. Common atom labeling scheme together with selected bond lengths (Å) and angles (°) for **7a**, **7b** and **8**.
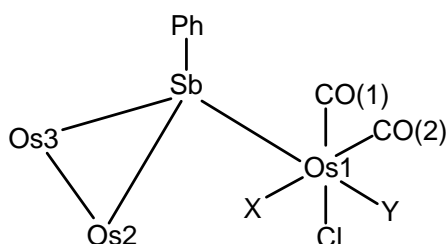
	7a	7b[†]	8[‡]
	X = CO; Y = Cl	X = Cl; Y = CO	X = CO; Y = Ph
Os2-Os3	2.9638(4)	2.9612(6)	2.9611(3); 2.9659(3)
Os1-Sb	2.6356(6)	2.6795(8)	2.7029(4); 2.7053(4)
Os2-Sb	2.6554(5)	2.6512(7)	2.6860(4); 2.6766(4)
Os3-Sb	2.6644(6)	2.6500(8)	2.6664(4); 2.6915(4)
Os1-X	3.097*	2.411(2)	3.086; 3.099*
Os1-Y	2.438(2)	3.094*	-
Os1-Cl	2.4315(19)	2.421(2)	2.4367(15); 2.4448(12)
Os1-CO(1)*	3.021	3.033	3.030; 3.022
Os1-CO(2)*	3.105	3.023	3.069; 3.082
Os2-Sb-Os3	67.713(15)	67.917(19)	67.177(11); 67.078(11)

[†]Two molecules in the asymmetric unit. Only bond parameters for ordered molecule given here.

[‡] Two molecules in the asymmetric unit. Values given are for molecules A and B, respectively.

*The values given are sum of the Os-C and C-O bond lengths.

The three clusters are closely related structurally; they comprise a spiked triangular Os_2Sb cluster, i.e., two Os-Os bonds have been cleaved. The spike in **7a** and **7b** comprise an

$Os(CO)_3Cl_2$ moiety; they are isomers differing in the coordination geometry about the spike (*mer* vs *fac* arrangements, respectively, of the carbonyls.) Cluster **8** is structurally similar to **7a**, with the Cl *trans* to the Sb replaced by a phenyl group. The Os1-CO(1) sum of bond lengths are short (~3.03 Å) for all the clusters as CO(1) is *trans* to a Cl, which is also the case for CO(2) in **7b**. Only two other osmium-antimony clusters, *viz.*, $Os_6(\mu_3\text{-}SbR)(\mu_3,\eta^2\text{-}C_6H_4)(CO)_{20}$ (R=Ph or Me), containing a μ_3-SbR fragment have previously been reported; both were obtained as minor products.[2f,g] Other related clusters containing a μ-ER fragment include the osmium-bismuth cluster $Os_2(CO)_8(\mu_2\text{-}BiPh)$, obtained in low yield from the reaction of **1** with $BiPh_3$,[19] and the osmium-tin cluster $Os_3(CO)_{12}(Ph)(\mu_3\text{-}SnPh)$.[20]

THF solutions of **7a** and **7b** were found to decompose slowly, presumably via substitution by THF at the $Os(CO)_3Cl_2$ fragment. This is presumably due to the presence of the two Cl ligands which increased the electrophilicity of the Os centre.[21] Consistent with this was the observation that **7** and **8** were not formed if THF was the reaction fsolvent. The structural similarity of **8** to **7a** also suggests that the former may have resulted from further reaction of the latter with $SbPhCl_2$. This would also be consistent with a stronger tendency towards cleavage of the phenyl group from the more electropositive Sb centre in $SbPhCl_2$ compared to $SbPh_2Cl$. Similar cleavage of a phenyl group from $SbPh_3$ has also been observed previously.[22] The reaction of **7b** and $SbPhCl_2$ under the similar conditions failed to give **8** even after a prolonged reaction time, however. Cluster **8** was also found not to show isomerisation analogous to that of **7a** to **7b**, even at an elevated temperature (55 °C).
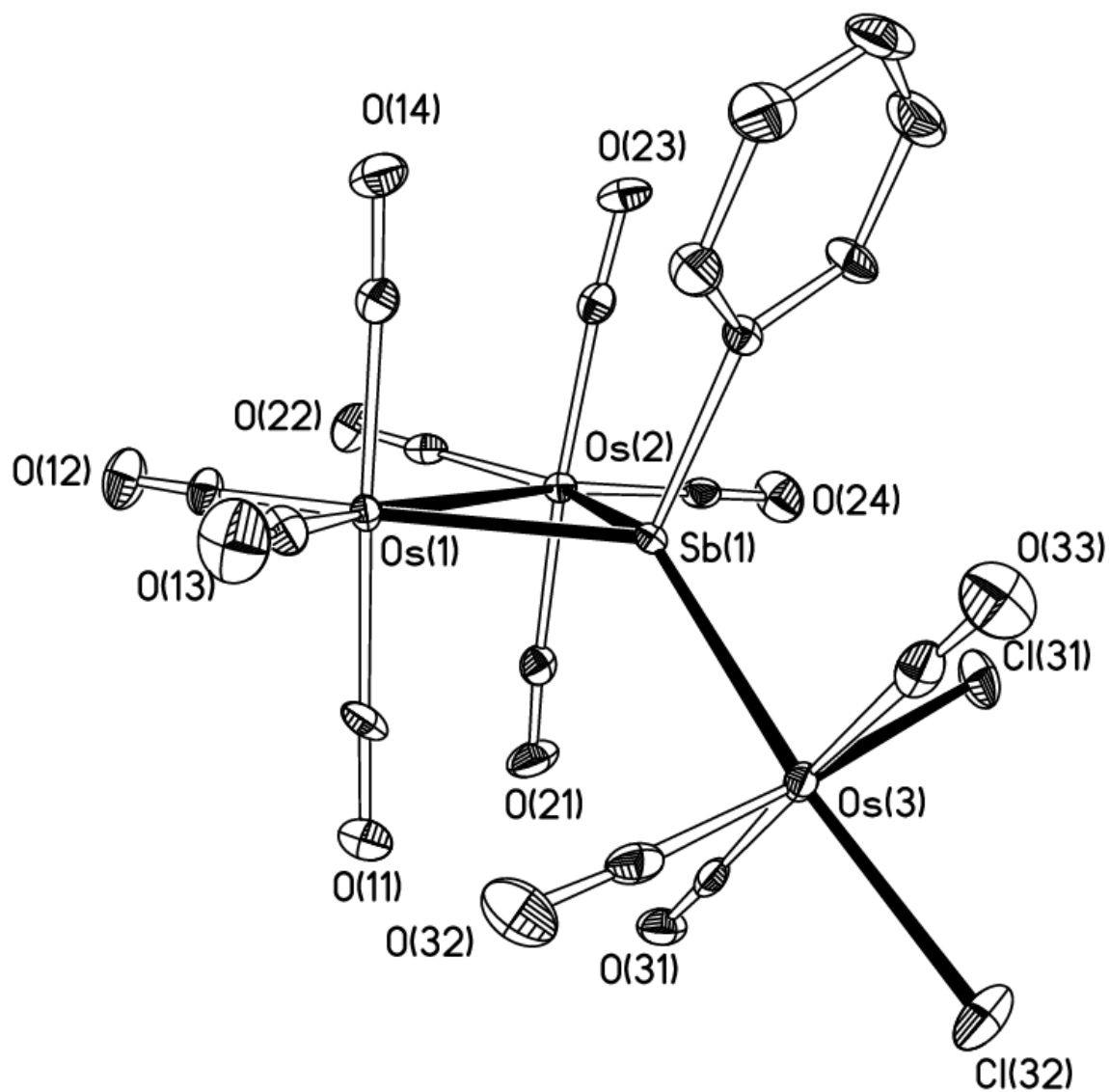
Figure 7. ORTEP diagram of the molecular structure of **7a**. Hydrogen atoms have been omitted and the thermal ellipsoids are drawn at the 50% probability level.
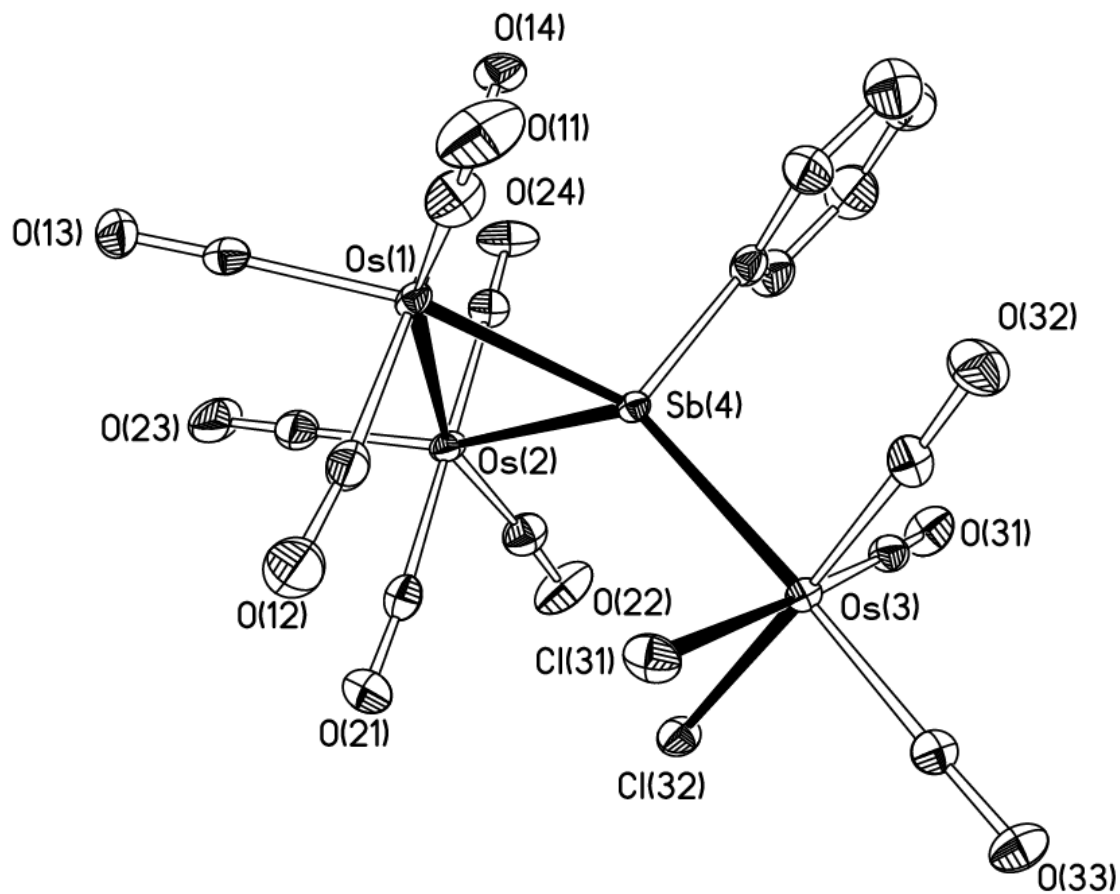
Figure 8. ORTEP diagram of the molecular structure of **7b**. Hydrogen atoms have been omitted and the thermal ellipsoids are drawn at the 50% probability level.
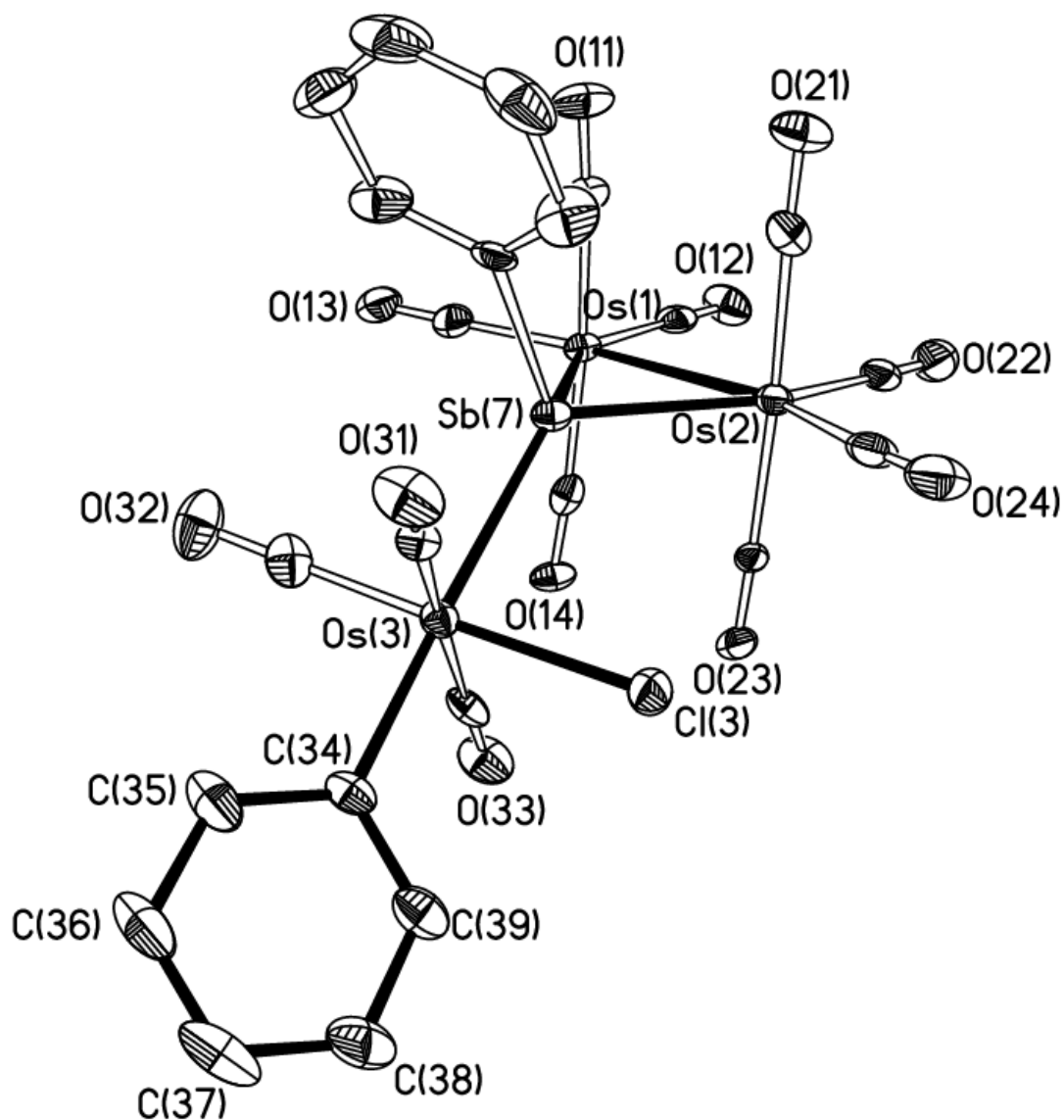
Figure 9. ORTEP diagram of the molecular structure of **8**. Hydrogen atoms have been omitted and the thermal ellipsoids are drawn at the 50% probability level.

The reaction pathway leading to these clusters is presumably similar to that for the reaction with SbPh$_2$Cl, i.e., via the substituted derivative Os$_3$(CO)$_{11}$(SbPhCl$_2$) to a cationic intermediate by nucleophilic displacement of a chloride (Scheme 3). Displacement of each chloride from antimony leads to cleavage of an Os-Os bond, thus resulting in the metal cores observed.
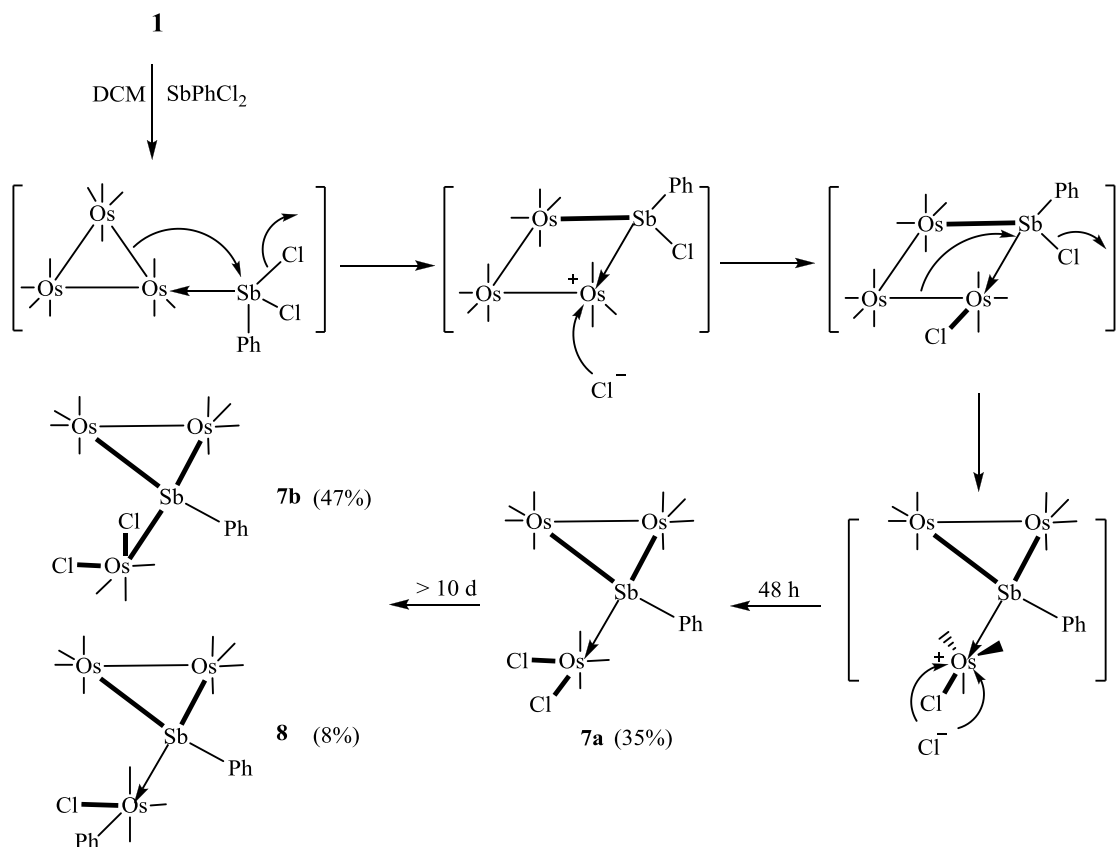
Scheme 3

Concluding remarks

In this work, we have described a facile approach to osmium-antimony clusters and rings via the binuclear oxidative addition of halostibines, exemplified by SbPh₂Cl and SbPhCl₂. The binuclear oxidative addition of each Sb-Cl bond led directly to cleavage of an Os-Os bond. The pathways for these reactions have been studied to various levels of detail, and the evidence suggested an ionic pathway. Compared to the hydrostibines (SbPh₂H) and distibines (Sb₂Ph₄), the halostibines were more readily available and stable, and the products from their reactions described here were not air- sensitive and thus easily separated by TLC. The halostibines would therefore serve as a more general synthetic route to such main group-transition element clusters

and rings. As these products carry halide ligands, they should also be amenable to further derivatisation, and expected to modify the reactivity of the metal centres.

Experimental section

General Data. All manipulations were carried out in an argon atmosphere with standard schlenk techniques. Reagent grade solvents were dried by the standard procedures and were freshly distilled prior to use. The clusters **1** and **2**,[23] and the halostibines $SbPh_2Cl$, $Sb(p\text{-tolyl})_2Cl$ and $SbPhCl_2$,[24] were prepared as described in the literature. TLC separations were carried out on 20 x 20 cm² plates coated with silica gel 60 F254, from Merck. NMR spectra were recorded on a 400 MHz NMR spectrometer; all chemical shifts were referenced to the residual proton resonance of the respective deuterated solvents. Mass spectra were recorded in ESI-ToF mode. Elemental analyses were carried out inhouse.

Reaction of 1 with SbPh₂Cl:

a) In Acetone: A sample of **1** (40 mg, 44 μmol) was dissolved in dry acetone (15 ml). To this was added $SbPh_2Cl$ (14 mg, 45 μmol). The resulting yellow mixture was stirred at room temperature for 48 h. The solvent was removed under reduced pressure and the residue separated by TLC with DCM/hexane (2:1, v/v) as the eluent to give two light yellow bands.

The first band was identified as $Os_3(CO)_{11}(Cl)(\mu\text{-}SbPh_2)$, **3b** ($R_f$ = 0.65; yield = 20 mg, 38%). IR (CH_2Cl_2): ν(CO) 2125m, 2087vs, 2063w, 2043vs, 2025m, 2013m, 1988w, 1970w cm⁻¹; ¹H NMR (C_6D_6) δ 7.66 (d, 2H, PhH), 7.55 (d, 2H, PhH), 6.88-7.06 (m, 6H, PhH). ¹³C{¹H} NMR ($CDCl_3$): δ 179.45 (1C, CO), 176.38 (1C, CO), 175.59 (1C, CO), 175.42(1C, CO), 174.09 (1C, CO), 173.95 (1C, CO), 173.63 (1C, CO), 172.16 (1C, CO), 168.76 (1C, CO), 168.19

(1C, CO), 164.79 (1C, CO), 136.61 (Ph), 135.06 (Ph), 130.30 (Ph), 129.54 (Ph), 129.28 (Ph), 128.41 (Ph), 126.27 (Ph), 125.47 (Ph). Anal. Calcd for $C_{23}H_{10}O_{11}ClOs_3Sb$: C 23.2, H 0.9. Found: C 23.6, H 0.8. ESI-MS$^+$ (*m/z*): 1210 [M+H$_2$O+H]$^+$, 1165 [M+H-CO]$^+$, 1126 [M+H$_2$O+H-3CO]$^+$, 1979 [M+H-4CO]$^+$, 1057 [M+H-5CO]$^+$.

The second band was an isomer **3a** (R_f = 0.40; yield = 25 mg, 48%). IR (CH$_2$Cl$_2$): ν(CO) 2125m, 2088vs, 2066s, 2040vs, 2022w, 2009w, 1989w cm^{-1}; ^{1}H NMR (C$_6$D$_6$) δ 7.35 (dd, 4H, PhH), 6.86-6.95 (m, 6H, PhH). Anal. Calcd for $C_{23}H_{10}O_{11}ClOs_3Sb$: C 23.2, H 0.9. Found: C 23.1, H 0.6. ESI-MS$^+$ (*m/z*): 1210 [M+H$_2$O+H]$^+$, 1165 [M+H-CO]$^+$, 1126 [M+H$_2$O+H-3CO]$^+$, 1057 [M+H-5CO]$^+$.

b) In DCM in the presence of Et$_4$NCl: A sample of **1** (30 mg, 32 μmol) and SbPh$_2$Cl (10 mg, 32 μmol) were dissolved in dry DCM (15 ml). The yellow mixture was stirred at room temperature for 12 h, resulting in the nearly full conversion into **A**, as determined from the IR spectrum. Et$_4$NCl (12 mg, 64μmol) was added and the resulting mixture was stirred at room temperature for another 36 h. The solvent was removed by rotary evaporation and the residue separated by TLC with DCM/hexane (2:1, v/v) as the eluent to give **3b** (R_f = 0.65; yield = 10 mg, 26%) and **3a** (R_f = 0.45; yield = 12 mg, 31%).

c) In DCM in the presence of Et$_4$NBr: Following a similar procedure as b) above, after the formation of **A**, Et$_4$NBr (7.0 mg, 33 μmol) was added and the mixture was stirred for another 4 h, leading to the complete consumption of **A** (by IR spectroscopy). After removal of the solvent followed by TLC separation with DCM/hexane (2:1, v/v) as the eluent, three bands were obtained.

The first band was identified as $Os_3(CO)_{11}(Br)(\mu\text{-SbPh}_2)$, **3c** ($R_f = 0.75$; yield = 18 mg, 46%).

IR (CH_2Cl_2): ν(CO) 2124m, 2086vs, 2063w, 2043vs, 2025m, 2013m, 1988w, 1970w cm^{-1}; ^{1}H

NMR (C_6D_6) δ 7.63 (d, 2H, PhH), 7.51 (d, 2H, PhH), 6.89-7.04 (m, 6H, PhH). ESI-MS$^+$ (m/z):

1254 [M+H$_3$O]$^+$, 1152 [M-Br]$^+$, 1079 [M+2H$_2$O-4CO-Br]$^+$, 1023 [M+2H$_2$O-6CO-Br]$^+$.

The other two bands were **3b** ($R_f = 0.65$; yield = 4.0 mg, 10%) and **3a** ($R_f = 0.45$; yield = 3.0 mg,

7.5%).

Conversion of 3b to 4: Cluster **3b** (20 mg, 17 μmol) was dissolved in 1, 2-dichloroethane (10

ml). The solution was heated to reflux for 12 h. After cooling, the solvent was removed under

reduced pressure, and the product was then separated by TLC using DCM/hexane (1:2, v/v) as

the eluent to yield a yellow band of $Os_3(CO)_{10}(\mu\text{-Cl})(\mu\text{-SbPh}_2)$, **4** ($R_f = 0.65$; yield = 15 mg,

77%). IR (Hexane): ν(CO) 2103s, 2064vs, 2055w, 2020s, 2014s, 1997s, 1983m cm^{-1}. ^{1}H NMR

(CDCl$_3$) δ 7.69-7.71 (q, 2H, PhH), 7.52-7.54 (q, 2H, PhH), 7.44-7.49 (m, 3H, PhH), 7.34-7.38

(m, 3H, PhH). ^{13}C{^{1}H} NMR (CDCl$_3$): 184.68 (2C, CO), 177.40 (1C, CO), 176.54 (1C, CO),

175.51 (2C, CO), 175.30 (2C, CO), 168.86 (2C, CO), 138.03 (Ph), 134.23 (Ph), 130.57 (Ph),

130.34 (Ph), 129.93 (Ph), 129.78 (Ph), 128.90 (Ph), 123.15 (Ph). Anal. Calcd for

$C_{22}H_{10}O_{10}ClOs_3Sb$: C 22.7, H 0.9. Found: C 22.7, H 0.6. ESI-MS$^+$ (m/z): 1223 [M+3H$_2$O+H]$^+$,

1168 [M+H]$^+$, 1139 [M+H-CO]$^+$, 1057 [M+3H$_2$O+H-4CO]$^+$, 1001 [M+3H$_2$O+H-6CO]$^+$.

Conversion of 3b to 5: To cluster **3b** (24 mg, 20 μmol) dissolved in dry THF (10 ml) was

added Na$_2$CO$_3$ (3.6 mg, 34 μmol) and deionized H$_2$O (0.5 ml). The resulting mixture was

stirred at room temperature for 72 h to give an orange solution. The solvent was removed and

the residue separated by TLC, with DCM/hexane (1:4, v/v) as the eluent, to give the known

cluster $Os_3(CO)_{10}(\mu\text{-H})(\mu\text{-SbPh}_2)$, **5**, as the only product (R_f = 0.40; yield = 16 mg, 69%), which was identified by its IR and ^1H NMR characteristics.[2a,b]

Reaction of 2 with SbPh$_2$Cl:

a) With one equivalent of SbPh$_2$Cl: To a sample of **2** (50 mg, 54 μmol) and SbPh$_2$Cl (17 mg, 54 μmol) placed in a carius tube was added dry DCM (10 ml). The solution was degassed by three cycles of freeze-pump-thaw and then heated at 55 °C for 36 h. TLC separation after removal of the solvent, with DCM/hexane (1:2, v/v) as the eluent, afforded a dark yellow band of **4** (R_f = 0.70; yield = 36 mg, 58%).

b) With two equivalents of SbPh$_2$Cl: A sample of **2** (50 mg, 54 μmol) and SbPh$_2$Cl (40 mg, 0.13 mmol) were dissolved in dry DCM (10 ml). The yellow mixture was stirred at room temperature for 72 h. The solvent was removed by rotary evaporation and the residue separated by TLC, with DCM/hexane (1:1, v/v) as the eluent, to give three bands. These were identified, in order of elution, to be yellow **4** (R_f = 0.90; yield = 4.0 mg, 6.5%), colorless $Os_3(CO)_{10}(Cl)_2(\mu\text{-SbPh}_2)_2$, **6b** ($R_f$ = 0.35; yield = 3.0 mg, 4.0%) and colorless **6a** (R_f = 0.25; yield = 18 mg, 22%).

A similar reaction in which the mixture was heated at 85 °C for 24 h gave, after TLC separation, colorless **6c** (R_f = 0.75; yield = 12.0 mg, 15%) and **6b** (R_f = 0.65; yield = 16 mg, 20%).

When the solvent was changed to dry THF (10 ml), and the mixture heated at 85 °C for 24 h, the product isolated was **6c** (R_f = 0.75; yield = 24.0 mg, 30%).

Cluster **6a**: IR (CH$_2$Cl$_2$): ν(CO) 2119m, 2101vs, 2073m, 2057s, 2035s, 2024s, 2008s cm^{-1}; ^1H NMR (C$_6$D$_6$) δ 7.91 (dd, 2H, PhH), 7.74 (dd, 2H, PhH), 7.58 (dd, 2H, PhH), 7.53 (dd, 2H, PhH), 6.96-7.07 (m, 12H, PhH). $^{13}C\{^1H\}$ NMR (CDCl$_3$): δ 186.13 (1C, CO), 183.57 (1C,

CO), 181.50 (1C, CO), 179.54 (1C, CO), 170.03 (1C, CO), 169.85 (1C, CO), 169.29 (1C, CO), 169.21 (1C, CO), 168.50 (1C, CO), 168.00 (1C, CO), 137.04 (Ph), 136.73 (Ph), 135.86 (Ph), 135.30 (Ph), 130.45 (Ph), 130.43 (Ph), 130.30 (Ph), 130.10 (Ph), 129.99 (Ph), 129.33 (Ph), 129.01 (Ph), 128.58 (Ph), 128.44 (Ph), 128.40 (Ph), 128.34 (Ph), 128.06 (Ph). Anal. Calcd for $C_{34}H_{20}O_{10}Cl_2Os_3Sb_2$: C 27.7, H 1.4. Found: C 27.7, H 1.4. ESI-MS$^+$ (m/z): 1492 [M+H$_3$O]$^+$, 1439 [M-Cl]$^+$, 1412 [M-Cl-CO]$^+$.

Cluster **6b**: IR (CH$_2$Cl$_2$, mixture of two isomers): ν(CO) 2118w, 2107vs, 2074s, 2050s, 2037s, 2016s, 1984m cm^{-1}; ^{1}H NMR (C$_6$D$_6$, mixture of two isomers) δ 8.27 (d, PhH), 7.98 (d, PhH), 7.93 (d, PhH), 7.72 (t, PhH), 7.63 (d, PhH), 7.57 (d, PhH), 6.92-7.25 (m, PhH). Anal. Calcd for $C_{34}H_{20}O_{10}Cl_2Os_3Sb_2$: C 27.7, H 1.4. Found: C 27.5, H 1.0. ESI-MS$^+$ (m/z): 1439 [M-Cl]$^+$, 1411 [M-Cl-CO]$^+$, 1383 [M-Cl-2CO]$^+$.

Cluster **6c**: IR (CH$_2$Cl$_2$): ν(CO) 2117s, 2099vs, 2072vs, 2048sh, 2038vs, 2009m, 1985w cm^{-1}; ^{1}H NMR (C$_6$D$_6$) δ 8.31 (d, 2H, PhH), 7.97 (d, 2H, PhH), 7.77 (d, 2H, PhH), 7.56 (d, 2H, PhH), 6.96-7.16 (m, 12H, PhH). ^{13}C{^{1}H} NMR (CDCl$_3$): δ 180.39 (1C, CO), 178.43 (1C, CO), 174.69 (1C, CO), 174.10 (1C, CO), 172.85 (1C, CO), 170.73 (1C, CO), 170.33 (1C, CO), 170.23 (1C, CO), 169.56 (2C, CO), 137.91 (Ph), 137.55 (Ph), 137.09 (Ph), 135.32 (Ph), 134.39 (Ph), 133.45 (Ph), 129.94 (Ph), 129.85 (Ph), 129.42 (Ph), 129.36 (Ph), 129.26 (Ph), 128.81 (Ph), 128.56 (Ph), 128.45 (Ph), 127.47 (Ph), 127.21 (Ph). Anal. Calcd for $C_{34}H_{20}O_{10}Cl_2Os_3Sb_2$: C 27.7, H 1.4. Found: C 27.7, H 1.2. ESI-MS$^+$ (m/z): 1492 [M+H$_3$O]$^+$, 1439 [M-Cl]$^+$, 1410 [M-Cl-CO]$^+$, 1382 [M-Cl-2CO]$^+$.

c) Synthesis of Tolyl-6b and Tolyl-6c: A mixture of **2** (50 mg, 54 μmol) and Sb(Tolyl)$_2$Cl (40 mg, 0.12 mmol) placed in a carius tube was dissolved in dry DCM (10 ml). After degassing with three cycles of freeze-pump-thaw, the mixture was heated at 85 °C for 24 h. The solvent was then removed and the residue separated by TLC, with DCM/hexane (1:1, v/v) as the eluent, to give two colorless bands.

The first band afforded Os$_3$(CO)$_{10}$(Cl)$_2$[μ-Sb(Tolyl)$_2$]$_2$, **Tolyl-6c** (R$_f$ = 0.85; yield = 10 mg, 12%). IR (CH$_2$Cl$_2$): ν(CO) 2115s, 2097vs, 2071vs, 2047sh, 2037vs, 2007m, 1984w cm^{-1}; ^{1}H NMR (C$_6$D$_6$) δ 8.27 (d, 2H, PhH), 7.94 (d, 2H, PhH), 7.75 (d, 2H, PhH), 7.55 (d, 2H, PhH), 7.05 (d, 2H, PhH), 6.92-7.00 (m, 6H, PhH), 2.04 (s, 3H, MeH), 2.03 (s, 3H, MeH), 2.02 (s, 3H, MeH), 1.97 (s, 3H, MeH).

The second band afforded **Tolyl-6b** (R$_f$ = 0.80; yield = 16 mg, 17%). IR (CH$_2$Cl$_2$): ν(CO) 2117w, 2106vs, 2072s, 2048s, 2036s, 2015s, 1983m cm^{-1}; ^{1}H NMR (C$_6$D$_6$, mixture of two isomers) δ 8.22 (d, PhH), 7.95 (d, PhH), 7.90 (d, PhH), 7.69-7.71 (dd, PhH), 7.60 (d, PhH), 7.56 (d, PhH), 7.24 (d, PhH), 7.06 (d, PhH), 6.84-6.98 (m, PhH), 2.01-2.03 (m, MeH), 1.96 (s, 3H, MeH) .

Conversion of 6b to 6c: Cluster **6b** (20 mg, 14 μmol) dissolved in dry THF (10 ml) was degassed (three freeze-pump-thaw cycles) and the solution heated at 85 °C for 12 h. After the solvent was removed under reduced pressure, TLC separation with DCM/hexane (2/1, v/v) as the eluent yield **6c** as the only separable product (R$_f$ = 0.75; yield = 17 mg, 85%).

Reaction of 1 with SbPhCl$_2$:

a) **Synthesis of 7a**: A sample of **1** (40 mg, 44 μmol) was dissolved in dry DCM (10 ml). To this was added SbPhCl$_2$ (12 mg, 44 μmol). The resulting yellow mixture was stirred at room temperature for 48 h. After removing the solvent, the residue was separated by TLC with DCM as the eluent, to give one major light yellow band of *mer*-Os$_3$(CO)$_{11}$(Cl)$_2$(μ_3-SbPh), **7a** (R$_f$ = 0.60; yield = 18 mg, 35%). IR (CH$_2$Cl$_2$): v(CO) 2142w, 2128s, 2101s, 2064vs, 2044w, 2035w, 2020w cm^{-1}. ^{1}H NMR (CDCl$_3$) δ 7.43-7.46 (q, 2H, PhH), 7.29-7.39 (m, 3H, PhH). ^{13}C{^{1}H} NMR (CDCl$_3$): δ 173.28 (2C, CO), 173.05 (2C, CO), 172.35 (2C, CO), 169.11 (2C, CO), 168.53 (2C, CO), 167.28 (1C, CO), 135.24 (Ph), 130.76 (Ph), 129.61 (Ph), 127.45 (Ph). Anal. Calcd for C$_{17}$H$_5$O$_{11}$Cl$_2$Os$_3$Sb: C 17.8, H 0.4. Found: C 17.6, H 0.4. ESI-MS$^+$ (*m/z*): 1168 [M+H$_2$O+H]$^+$, 1140 [M+H$_2$O+H-CO]$^+$, 1085 [M+H$_2$O+H-3CO]$^+$, 1057 [M+H$_2$O+H-4CO]$^+$.

b) **Synthsis of 7b and 8**: TLC separation of a similar reaction as above, with **1** (120 mg, 0.13 mmol) and SbPhCl$_2$ (36 mg, 0.13 mmol) in dry DCM (30 ml) for 10 days, afforded two bands:

The first, colorless, band was *mer*-Os$_3$(CO)$_{11}$(Cl)(Ph)(μ_3-SbPh), **8** (R$_f$ = 0.75; yield = 6.0 mg, 7.7%). IR (CH$_2$Cl$_2$): v(CO) 2135m, 2112m, 2095s, 2053vs, 2042w, 2031w, 1989w cm^{-1}. ^{1}H NMR (CD$_2$Cl$_2$) δ 7.75 (dd, 2H, PhH), 7.51 (dd, 2H, PhH), 7.26-7.34 (m, 3H, PhH), 7.00-7.09 (m, 3H, PhH). ^{13}C{^{1}H} NMR (CD$_2$Cl$_2$): δ 182.22 (1C, CO), 179.43 (2C, CO), 174.47 (2C, CO), 174.18 (2C, CO), 172.44 (2C, CO), 170.13 (1C, CO), 141.72 (Ph), 136.05 (Ph), 129.55 (Ph). 128.98 (Ph), 128.36 (Ph), 127.36 (Ph), 126.32 (Ph), 124.08 (Ph). Anal. Calcd for C$_{23}$H$_{10}$O$_{11}$ClOs$_3$Sb: C 23.2, H 0.9. Found: C 23.10, H 0.6. ESI-MS$^+$ (*m/z*): 1210 [M+H$_2$O+H]$^+$, 1128 [M+H$_2$O+H-3CO]$^+$, 1087 [M+H-Ph-CO]$^+$, 1057 [M+H-Ph-2CO]$^+$.

The second, very light yellow, band was fac-$Os_3(CO)_{11}(Cl)_2(\mu_3$-SbPh), **7b** ($R_f$ = 0.50; yield = 70 mg, 47%), an isomer of **7a**. IR (CH_2Cl_2): $\nu(CO)$ 2139w, 2113s, 2103s, 2056vs, 2030w, 2016w cm^{-1}. ^1H NMR ($CDCl_3$) δ 7.53-7.55 (q, 2H, PhH), 7.29-7.36 (m, 3H, PhH).$^{13}C\{^1H\}$ NMR ($CDCl_3$): δ 173.70 (2C, CO), 170.71 (2C, CO), 170.19 (2C, CO), 168.71 (2C, CO), 167.94 (2C, CO), 164.84 (1C, CO), 136.31 (Ph), 130.14 (Ph), 129.34 (Ph), 127.53 (Ph). Anal. Calcd for $C_{17}H_5O_{11}Cl_2Os_3Sb$: C 17.8, H 0.4. Found: C 17.6, H 0.2. ESI-MS$^+$ (m/z): 1168 [M+H$_2$O+H]$^+$, 1140 [M+H$_2$O+H-CO]$^+$, 1085 [M+H$_2$O+H-3CO]$^+$, 1057 [M+H$_2$O+H-4CO]$^+$.

Crystallographic analyses. Light yellow crystals of **3b, 3c, 4, 6a, 6b, Tolyl-6b, 6c, Tolyl-6c, 7b** and **8**, suitable for X-ray diffraction analyses were obtained by slow evaporation of solvent from solutions in hexane/methylene chloride solvent mixtures at room temperature; Light yellow crystals of metastable **3a** were obtained by directly evaporating the mixture of **1** and SbPh$_2$Cl (1:1 mole ratio) in THF at -30 °C under an inert atmosphere, and light yellow crystals of metastable **7a** were obtained by slow evaporation from a dichloromethane solution at -30 °C. Each crystal was glued onto the end of a thin glass fibre. For clusters **3b, 4, 6a, 6b, Tolyl-6b, 6c, Tolyl-6c, 7a** and **7b**, the X-ray diffraction intensity data were collected on a Bruker Kappa diffractometer equipped with a CCD detector, employing Mo Kα radiation (λ = 0.71073 Å), with the SMART suite of programs;[25] all the data were processed and corrected for Lorentz and polarization effects with SAINT and for absorption effects with SADABS.[26] For clusters **3a, 3c** and **8**, the intensity data were collected on a SuperNova (Dual source) Agilent diffractometer using Mo Kα radiation (λ = 0.71073 Å); the data were processed and corrected for absorption effects with CrysAlisPro.[27] All the structural solutions and refinements were carried out with the

SHELXTL suite of programs.[28] All non-hydrogen atoms were refined with anisotropic thermal parameters. Crystal data, data collection parameters, and refinement data are summarized in Table S1.

Two crystallographically independent molecules were found in the crystals of **7b** and **8**. There were disorder observed for **6b**, **Tolyl-6b**, **6c**, **Tolyl-6c** and one molecule in **7b**. For **6b**, this was interpreted as comprising two stereoisomers, with one of them exhibiting disorder about a two-fold rotation axis that passes through the unique Os. The disorder in **Tolyl-6b** was also interpreted as comprising two stereoisomers present in a ratio of about 2:3; this was consistent with the ^{1}H NMR data. The disorder in **6c, andTolyl-6c** were about a two-fold rotation axis that passes through the unique Os, with occupancy ratios of 3:2 and 1:1, respectively. The disorder in **7b** was of the phenyl and the Cl ligands, which were modeled with two sites each of occupancies 55:45. A THF solvate was found in the crystal of **3a**, and DCM in the crystals of **6a**, **6c** and **Tolyl-6c**. The DCM solvates were disordered and modeled as about a centre of inversion in **6a**, and with four orientations in the other two.

Computational details. DFT calculations were performed with the Gaussian 09W suite of programs,[29] utilizing Becke's three-parameter hybrid function and Lee–Yang–Parr's gradient-corrected correlation function (B3LYP).[30] The LanL2DZ (Los Alamos effective core potential double-ζ) basis set, together with d- or f-type polarization functions,[31] is employed for the Os and Sb atoms while the 6-311+G(2d, p) basis set is used for the remaining atoms. Spin-restricted calculations were used for geometry optimization. Harmonic frequencies were then

calculated to characterize the stationary points as equilibrium structures with all real frequencies, and to evaluate zero-point energy (ZPE) corrections.

Supporting Information

Tables and CIF files containing the crystallographic data of all the new structures; ^{1}H, ^{13}C{^{1}H} NMR, IR and MS spectra of all the new structures; the IR comparison spectra between **A** and $Os_3(CO)_{11}(SbPh_3)$; the IR comparison spectra between **3b** and **3c**; the ^{1}H NMR monitoring spectra of the conversion of **3a** to **3b**, **7a** to **7b**, **6a** to **6c**; the ^{1}H EXSY spectrum for **Tolyl-6b**; the monitoring reactions of **1** and **4** with SbPh$_2$Cl, respectively; all the computationally optimized structures of **3a**, **3b**, **6a**, **6b-1**, **6b-2**, **6c**, **7a** and **7b**, with the corresponding optimized coordinates and free energies. This material is available free of charge via the Internet at http://pubs.acs.org."

REFERENCES

1. For selected reviews, see: a) J. N. Nicholls, *Polyhedron* **1984**, 3, 1307. b) W. A. Herrmann, *Angew. Chem., Int. Ed. Engl.* **1986**, 25, 56. c) T. P. Fehlner, *Inorganometallic Chemistry*, Plenum, New York, 1992. d) K. H. Whitmire, *Adv. Organomet. Chem.* **1998**, 42, 1.

2. a) Colbran, S. B.; Irele, P. T.; Johnson, B. F. G.; Lahoz, F. J.; Lewis, J.; Raithby, P. R., *J. Chem. Soc., Dalton Trans.* **1989**, 2023. b) Chen, G. Z.; Leong, W. K., *J. Chem. Soc., Dalton Trans.* **1998**, 2489. c) Chen, G.; Leong, W. K., *J. Organomet. Chem.* **1999**, *574*, 276. d) Leong, W. K.; Chen, G., *J. Chem. Soc., Dalton Trans.* **2000**, 4442. e) Leong, W. K.; Chen, G., *Organometallics* **2001**, *20*, 2280. f) Chen, G. Z.; Leong, W. K., *J. Clust. Sci.* **2006**, *17*, 111. g) Chan, K. H.; Leong, W. K.; Mak, K. H. G., *Organometallics* **2006**, *25*, 250.

3. Li, Y.-Z.; Ganguly, R.; Leong, W. K., *Organometallics* **2014**, *33*, 823.

4. a) Ernst, R. D.; Marks, T. J.; Ibers, J. A., *J. Am. Chem. Soc.* **1977**, *99*, 2090. b) Röttinger, E.; Müller, R.; Vahrenkamp, H., *Angew. Chem. Int. Ed.* **1977**, *16*, 332. c) Leong, W. K.; Einstein, F. W. B.; Pomeroy, R. K., *Organometallics* **1996**, *15*, 1582. d) Leong, W. K.; Pomeroy, R. K.; Batchelor, R. J.; Einstein, F. W. B.; Campana, C. F., *Organometallics* **1997**, *16*, 1079. e) Adams, R. D.; Pearl, W. C., *Inorg. Chem.* **2009**, *48*, 9519. f) Raja, R.; Adams, R. D.; Blom, D. A.; Pearl, W. C.; Gianotti, E.; Thomas, J. M., *Langmuir.* **2009**, 25, 7200. g) Adams, R. D.; Pearl, W. C., *Inorg. Chem.* **2010**, 49, 6188. h) Adams, R. D.; Pearl Jr, W. C., *J. Organomet. Chem.* **2010**, 695, 937c.

5. a) Benjamin, S. L.; Levason, W.; Reid, G.; Warr, R. P., *Organometallics* **2012**, *31*, 1025. b) Ke, I.-S.; Gabbaï, F. P., *Inorg. Chem.* **2013**, *52*, 7145.

6. a) Benlian, D.; Bigorgne, M., *Bull. Soc. Chim. Fr.* **1963**, 1583. b) Breunig, H. J.; Fichtner, W., *Z. Anorg. Allg. Chem.* **1981**, *477*, 119. c) Herberhold, M.; Schamel, K., *Z. Naturforsch.* **1988**, *43b*, 1274. d) Graf, N.; Wieber, M., *Z. Anorg. Allg. Chem.* **1993**, *619*, 2061. e) Wieber, M.; Graf, N., *Z. Anorg. Allg. Chem.* **1993**, *619*, 1991. f) Breunig, H. J.; Borrmann, T.; Lork, E.; Raţ, C. I., *J. Organomet. Chem.* **2007**, *692*, 2593.

7. Leong, W. K., *M. Sc. Thesis*, National University of Singapore **1992**.

8. Yamashita, H.; Kawamoto, A. M.; Tanaka, M.; Goto, M., *Chem. Lett.* **1990**, 2107.

9. Janzen, M. C.; Jennings, M. C.; Puddephatt, R. J., *Organometallics* **2001**, *20*, 4100.

10. Clegg, W.; Lawlor, F. J.; Lesley, G.; Marder, T. B.; Norman, N. C.; Orpen, A. G.; Quayle, M. J.; Rice, C. R.; Scott, A. J.; Souza, F. E. S., *J. Organomet. Chem.* **1998**, *550*, 183.

11. Yamashita, H.; Kobayashi, T.; Tanaka, M.; Samuels, J. A.; Streib, W. E., *Organometallics* **1992**, *11*, 2330.

12. a) Butler, G.; Eaborn, C.; Pidcock, A., *J. Organomet. Chem.* **1979**, *181*, 47. b) Clark, H. C.; Davies, J. A., *J. Organomet. Chem.* **1981**, *213*, 503. c) Holt, M. S.; Wilson, W. L.; Nelson, J. H., *Chem. Rev.* **1989**, *89*, 11. d) Nelson, J. H.; Wilson, W. L.; Cary, L. W.; Alcock, N. W.; Clase, H. J.; Jas, G. S.; Ramsey-Tassin, L.; Kenney, J. W., *Inorg. Chem.* **1996**, *35*, 883. e) Farkas, E.; Kollar, L.; Moret, M.; Sironi, A., *Organometallics* **1996**, *15*, 1345. f) Al-Allaf, T. A. K., *J. Organomet. Chem.* **1999**, *590*, 25. g) van der Veen, L. A.; Keeven, P. K.; Kamer, P. C. J.; van Leeuwen, P. W. N. M., *J. Chem. Soc., Dalton Trans.* **2000**, 2105. h) Teles, W. M.; Speziali, N. L.; Filgueiras, C. A. L., *Polyhedron* **2000**, *19*, 739.

13. Conole, G.; Hill, K. A.; McPartlin, M.; Mays, M. J.; Morris, M. J., *J. Chem. Soc., Chem. Commun.* **1989**, 688.

14. Braunschweig, H.; Brenner, P.; Cogswell, P.; Kraft, K.; Schwab, K., *Chem. Commun.* **2010**, *46*, 7894.

15. Crabtree, R. H., The Organometallic Chemistry of the Transition Metals; Wiley-Interscience, 2005, pp.159–180.

16. a) Leong, W. K.; Einstein, F. W. B.; Pomeroy, R. K., *J. Cluster Sci.* **1996**, *7*, 121. b) Leong, W. K.; Leong, W. L. J.; Zhang, J., *J. Chem. Soc., Dalton Trans.* **2001**, 1087. c) Chen, G.; Deng, M.; Lee, C. K.; Leong, W. K., *Organometallics* **2002**, 21, 1227. d) Chen, G.; Deng, M.; Lee, C. K. D.; Leong, W. K.; Tan, J. L.; Tay. C. T., *J. Organomet. Chem.* **2006**, *691*, 387.

17. Johnson, B. F. G.; Lewis, J.; Whitton, A. J.; Bott, S. G., *J. Organomet. Chem.*, **1990**, *389*, 129.

18. Leong, W. K.; Chen, G. Z., *Organometallics* **2001**, *20*, 5771.

19. Adams, R. D.; Pearl, W. C., Jr., *Inorg. Chem.* **2010**, *49*, 7170.

20. Adams, R. D.; Captain, B.; Zhu, L., Organometallics **2006**, *25*, 4183.

21 . a) Kuhlman, R.; Streib, W. E.; Huffman, J. C.; Caulton, K. G., *J. Am. Chem. Soc.* **1996,** *118*, 6934. b) Clark, H. C. S.; Coleman, K. S.; Fawcett, J.; Holloway, J. H.; Hope, E. G.; Redding, J.; Russell, D. R., *Polyhedron* **1999**, *18*, 1207. c) Mondal, N.; Das, P.; Roy, B.; Ghosh, B., *Transit. Metal Chem.* **1999,** *24*, 678. d) Barton, A. J.; Levason, W.; Reid, G.; Tolhurst, V.-A., *Polyhedron* **2000,** *19,* 235.

22. Adams, R. D.; Captain, B.; Pearl Jr, W. C., *J. Organomet. Chem.* **2008,** *693*, 1636.

23. a) Johnson, B. F. G.; Lewis, J.; Pippard, D. A., *J. Chem. Soc., Dalton Trans.* **1981**, 407. b) J. N. Nicholls, Vargas, M. D., *Inorg. Synth.* **1990**, *28*, 232.

24. Nunn, M.; Sowerby, D. B.; Wesolek, D. M., *J. Organomet. Chem.* **1983**, *251,* C45.

25. SMART version 5.628; Bruker AXS Inc.: Madison, WI, USA, **2001**.

26. Sheldrick, G. M., SADABS, **1996.**

27. Agilent Technologies, *CrysAlisPro*, Version 1.171.35.21b.

28. SHELXTL version 5.1; Bruker AXS Inc.: Madison, WI, USA, **1997**.

29. Gaussian 09, Revision D.01, Frisch, M. J.; Trucks, G. W.; Schlegel, H. B.; Scuseria, G. E.; Robb, M. A.; Cheeseman, J. R.; Scalmani, G.; Barone, V.; Mennucci, B.; Petersson, G. A.; Nakatsuji, H.; Caricato, M.; Li, X.; Hratchian, H. P.; Izmaylov, A. F.; Bloino, J.; Zheng, G.; Sonnenberg, J. L.; Hada, M.; Ehara, M.; Toyota, K.; Fukuda, R.; Hasegawa, J.; Ishida, M.; Nakajima, T.; Honda, Y.; Kitao, O.; Nakai, H.; Vreven, T.; Montgomery, J. A., Jr.; Peralta, J. E.; Ogliaro, F.; Bearpark, M.; Heyd, J. J.; Brothers, E.; Kudin, K. N.; Staroverov, V. N.; Kobayashi, R.; Normand, J.; Raghavachari, K.; Rendell, A.; Burant, J. C.; Iyengar, S. S.; Tomasi, J.; Cossi, M.; Rega, N.; Millam, N. J.; Klene, M.; Knox, J. E.; Cross, J. B.; Bakken, V.; Adamo, C.; Jaramillo, J.; Gomperts, R.; Stratmann, R. E.; Yazyev, O.; Austin, A. J.; Cammi, R.; Pomelli, C.; Ochterski, J. W.; Martin, R. L.; Morokuma, K.; Zakrzewski, V. G.; Voth, G. A.; Salvador, P.; Dannenberg, J. J.; Dapprich, S.; Daniels, A. D.; Farkas, Ö.; Foresman, J. B.; Ortiz, J. V.; Cioslowski, J.; Fox, D. J. Gaussian, Inc., Wallingford CT, 2009.

30. Lee, C.; Yang, W.; Parr, R. G., *Phys. Rev. B* **1988**, *37*, 785.

31. a) *Gaussian Basis Sets for Molecular Calculations*, Huzinaga, S.; Andzelm, J., Elsevier: Amsterdam; **1984**, p. 23 b) Ehlers, A. W.; Böhme, M.; Dapprich, S.; Gobbi, A.; Höllwarth, A.; Jonas, V.; Köhler, K. F.; Stegmann, R.; Veldkamp, A.; Frenking, G., *Chem. Phys. Lett.* **1993**, *208*, 111.